Effect of annealing on thermal and dynamic mechanical properties of poly(lactic acid)

Assia Zennaki, Latifa Zair, Khadidja Arabeche, Lina Benkraled, Ulrich Maschke, Abdelkader Berrayah

Received: 13 July 2022 | Revised: 4 August 2022 | Accepted: 8 August 2022

DOI: 10.1002/app.53095

RESEARCH ARTICLE

Applied Polymer SCIENCE WILEY

Effect of annealing on thermal and dynamic mechanical properties of poly(lactic acid)

Assia Zennaki[1] | **Latifa Zair**[1] | **Khadidja Arabeche**[1] | **Lina Benkraled**[1] | **Ulrich Maschke**[2] | **Abdelkader Berrayah**[1]

[1]Laboratoire de Recherche sur les Macromolécules, Faculté des Sciences, Université Aboubakr Belkaïd, Tlemcen, Algeria

[2]UMET – Unité Matériaux et Transformations, UMR 8207, University of Lille, CNRS, INRAE, Centrale Lille, Lille, France

Correspondence
Ulrich Maschke, UMET – Unité Matériaux et Transformations, UMR 8207, University of Lille, CNRS, INRAE, Centrale Lille, Lille F-59000, France.
Email: ulrich.maschke@univ-lille.fr

Funding information
University of Lille/France; Centre National de la Recherche Scientifique (CNRS); University of Tlemcen/Algeria; General Directorate of Scientific Research and Technological Development (DGRSDT); Algerian Ministry of Higher Education and Scientific Research (MESRS)

Abstract

Effects of annealing temperature (T_a: 80–140°C) and time (t_a: 3-30 h) on the crystalline phase transition in poly(lactic acid) (PLA) were studied by differential scanning calorimetry (DSC) and dynamic mechanical analysis (DMA). In the DSC curves, the sample annealed at $T_a = 80$°C with time interval (t_a: 10–30 h) demonstrates a peculiarly small exothermal peak (T_{exo}) around 130°C, just prior to the melting point, corresponding to the disorder-to-order (α'-to-α) phase transition, while the sample annealed at temperature (T_a: 90–110°C) shows a double melting behavior considered as the α'-α phase transition. Towards low temperatures, the glass modulus E_g reported by DMA thermograms, shows an important increase (~30,000 MPa) at $T_a = 80$°C for $t_a = 3$ h, due to the extremely high self-nucleation density in low-crystallized PLA materials. After a sharp drop to 3600 MPa at $T_a = 110$°C, a marked improvement of E_g (15,900 MPa) is observed around $T_a = 120$°C for all samples, regardless of time t_a. This interesting effect (improvement of E_g in the range $T_a = 100$–120°C) can be correlated with the grow of crystallinity in the same domain of T_a, and the α'-α phase transition T_a (T_a: 90–110°C) determined by the double T_m melting DSC peak, which is confirmed by the increase of T_g for $T_a = 90$–110°C.

KEYWORDS

biodegradable, crystallization, glass transition, mechanical properties, thermal properties

1 | INTRODUCTION

Poly(lactic acid) (PLA) is a biodegradable plastic, derived from renewable resources; it is a material of choice[1–7] in applications of various domains such as biomedicine, food packaging, textile, electronics, and so forth. PLA is characterized by slow crystallization kinetics often observed in conventional processing methods (extrusion, injection, etc.). This phenomenon is highly problematic, with significant consequences on thermal and mechanical properties of the final product. In many applications, increasing the crystallinity of PLA is desired because, in its amorphous form, the field of application of PLA is severely limited by its low glass transition temperature

(T_g). At temperatures higher than T_g, only the crystalline phase of PLA can impart valuable mechanical properties. Thus, the crystalline form is necessary to increase the strength of the material.[8–11] Annealing is widely used for the recrystallization of PLA-based materials.[12–15] Improvement of thermo-mechanical properties is sometimes obtained by mixing PLAs of different molar masses or with other biodegradable polymers.[16,17]

Typically, PLA homopolymer has three crystal forms,[8,9,18–20] such as α-, β-, and γ-form, which depend on the crystallization conditions. Among all these crystal forms, the α-form is the most common and stable polymorph. It has been shown that PLA is polymorphic,[21–26] exhibiting two different crystalline phases termed α and α'. Crystallization of the relaxed melt at temperatures above 120°C leads to the formation of α-crystals with a 10_3 helical chain conformation where two chains are interacting in an orthorhombic unit cell.[18,27,28] At temperatures lower than 100°C only α'-crystals develop. In the α'-form, the molecule segments adopt the same helical structure as in α-crystals, however they exhibit conformational disorders.[28] Within the 100–120°C crystallization temperature range, a mixture of crystalline phases α' and α was present. The α'-crystals are metastable at their formation temperature but transform into the stable α-form upon heating at their stability limit of around 150°C.[21–23,28–32] Zhang and coauthors[29,30] confirmed that the small exothermic peak T_{exo} in the DSC curve, detected just prior to the melting peak, is associated with the disorder-to-order (α' to α) phase transition. This exothermic signal, already reported by Ohtani et al.,[33] Chao et al.[34] and Zhao et al.,[35] has been confirmed by Zhang and coauthors[29,30] by DSC, WAXD, and IR techniques. In the DSC thermograms, two endothermic peaks appear, related to the melting of the α' and α phases. The peak at the lower temperature is related to the melting of the α' -form and its recrystallization into the α form, while the second peak corresponds to the melting of the α-form. The two processes, the melting of the α' form and the recrystallization into the α form, can be considered as the α'-α phase transition.

This study aims to understand the fundamental effect of annealing time t_a and temperature T_a on the thermal and mechanical behavior of PLA. The α'-α phase diagram as function of t_a and T_a was determined by melting peaks from DSC data. Crystallinity of annealed PLA as a function of T_a for different t_a will be determined and correlated with the α'-α phase diagram. Through the DMA data, the glass modulus E_g and loss tangent tan δ of annealed PLA, as a function of T_a for different t_a, was determined and analyzed for particular conditions of T_a and t_a. Correlation between α'-α phase transition and crystallinity, mechanical properties (E_g) and molar mass (M_v) will be discussed.

2 | EXPERIMENTAL

2.1 | Materials

The poly(lactic acid), supplied by Nature Works (USA), was a semi-crystalline 4043D grade material comprising around 4% mol of D-isomer units. The PLA pellets were transparent and amorphous.

2.2 | Sample preparation

Poly(lactic acid) (PLA) granules were dried in a vacuum oven at 50°C for 24 h, then melted at 200°C and compressed into a sheet with a thickness of about 1 mm. The melted-compressed PLA sheet was immediately quenched into ice water to obtain an amorphous PLA sheet. Amorphous PLA is then annealed in a vacuum oven, at temperatures T_a: between 80 and 140°C, and time t_a between 3 and 30 h. In the present study, the PLA samples of un-annealed (amorphous) and annealed at different T_a and t_a are referred to as "un-aPLA" and "aPLA" (T_a; t_a); for example, aPLA ($T_a = 80$°C; $t_a = 30$ h) means annealed sheet at 80°C and 30 h.

2.3 | Molecular weight measurement

The molecular weight of PLA was determined from its intrinsic viscosity (η) measurement applying the Mark-Houwink equation, using an Ubbelohde-type capillary viscometer at 25°C. Chloroform was used as solvent. The viscosity average molecular weight M_v was calculated from the intrinsic viscosity by using the following equation[36]:

$$[\eta] = 5.45 \times 10^{-4} M_v^{0.73} \quad (1)$$

2.4 | Thermal analysis

Differential scanning calorimetry (DSC) measurements were performed on a TA Q2000 DSC apparatus equipped with a Refrigerated Cooling System (RCS90) allowing cooling down to −90°C. Temperature and heat flow scales were calibrated with high purity indium standards. Hermetic aluminum pans (Tzero, TA Instruments) were used, which are able to stand an internal pressure of 300 kPa. Samples of about 10 mg were analyzed under nitrogen gas flow at a heating rate of 10°C/min from 25 to 200°C, kept at the latter temperature for 2 min; cooled back to 25°C, followed by an isothermal scan for 2 min. The crystallinity rate (X_c) induced by the thermal treatment could be deduced from the heat flow signal obtained by DSC, using the following equation[37]:

$$Xc = \frac{\Delta H_m - \Delta H_c}{\Delta H_c^0} \quad (2)$$

where ΔH_m and ΔH_C are the enthalpies of melting and crystallization of the PLA samples, respectively, and ΔH_c^0 represents the enthalpy of fusion of the PLA crystal of infinite size, which was reported by Fischer et al.[38] to be 93.1 (J/g).

2.5 | Dynamic mechanical analysis

For the study of viscoelastic phenomena, dynamic stresses are used in the frequency domain rather than in the time domain. The method consists of applying a sinusoidal deformation $\varepsilon(t) = \varepsilon_0 \sin(\omega t)$ of low amplitude ε_0 to the material and measuring the resulting sinusoidal stress $\sigma(t)$ of amplitude σ_0. For a viscoelastic material, $\sigma(t)$ is out of phase by a loss angle δ ($0 \geq \delta \geq \pi/2$) with respect to the deformation:

$$\begin{aligned}\sigma(t) &= \sigma_0 \sin(\omega t + \delta) \\ &= \left[\frac{\sigma_0 \cos\delta}{\varepsilon_0}\right] \varepsilon_0 \sin(\omega t) + \left[\frac{\sigma_0 \sin\delta}{\varepsilon_0}\right] \varepsilon_0 \cos(\omega t) \\ &= E' \varepsilon_0 \sin(\omega t) + E'' \varepsilon_0 \cos(\omega t) \\ &= E' \varepsilon_0 \sin(\omega t) + E'' \varepsilon_0 \sin\left(\omega t + \frac{\pi}{2}\right)\end{aligned} \quad (3)$$

$E'(\omega)$, the modulus of conservation in phase with the deformation, characterizes the energy stored in the sample in elastic form. $E''(\omega)$, the phase shifted loss modulus of $\pi/2$ with the deformation, characterizes the energy dissipated in the sample in viscous form. Tan $\delta = E''/E'$ is defined as the loss tan.

In general, storage moduli E' versus temperature, at a given frequency ω, present a plateau exhibiting high values (around 10^9 Pa) towards low temperatures, defined by E_g, the storage modulus in the glassy region. With increasing temperature, E' drops sharply towards about 10^5 Pa; this sudden drop, defined by the glass transition zone, is characterized by the T_g which is defined by the peak of tan $\delta = E''/E'$ versus temperature.

Dynamic mechanical analysis was performed using a DMA Q800 (TA, Inc.). Experiments were conducted in tensile mode at a frequency of 1 Hz. Curves displaying storage (E') and loss (E'') moduli were recorded as a function of temperature between 25 and 180°C applying a heating rate of 3°C/min. The amplitude and the preload force were 5 μm and 0.010 N, respectively. The shape of the PLA films was rectangular, with dimensions $10 \times 6 \times 1$ mm^3. The temperatures of various relaxation processes were determined from the tan δ temperature curve at 1 Hz. The glass transition temperature (T_g) can be defined as the maximum of the transition in the loss tangent curve.

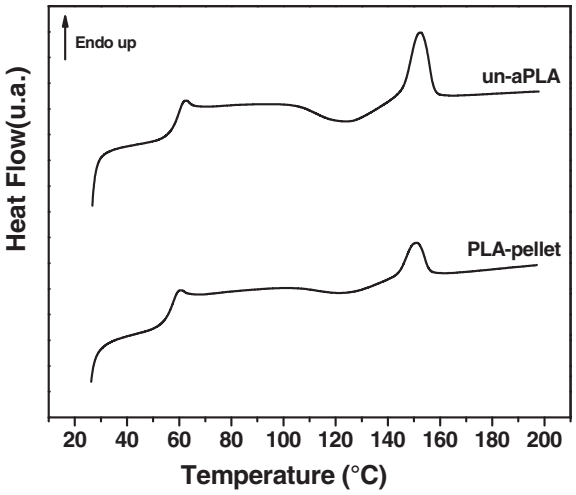

FIGURE 1 DSC thermograms of as-received poly(lactic acid) (PLA)-pellet and the un-aPLA sheet

3 | RESULTS AND DISCUSSION

3.1 | DSC analysis

Figure 1 illustrates a comparison of DSC thermograms of the as-received PLA-pellet dried in a vacuum oven at 50°C and the un-annealed sample (un-aPLA), taken as reference sample for all thermograms. un-aPLA exhibits amorphous behavior with a very low crystallinity rate ($X_c = 1.6\%$) and a glass transition at 60°C. An exothermic peak T_{cc} associated with a cold crystallization process appears at 127.2°C, following by an endotherm event with a central peak at $T_m = 153.4$°C. The results from thermal analysis of un-aPLA sample and PLA-pellets are given in Table 1.

DSC curves of aPLA (T_a: 80–140°C; t_a: 3–30 h) samples were analyzed. Annealing PLA samples at 80°C and times t_a: 3–30 h were illustrated in Figure 2. The small exothermal peak T_{exo}, just prior to the melting point, associated with the disordered-order α'-α phase transition, clearly appears for t_a = 10-30 h. This exothermal event, previously reported by Zhang et al.,[31] was found to be in agreement with reports from many authors.[20–28] Thermal properties of aPLA ($T_a = 80$°C; $t_a = 3$ h) sample were given in Table 2.

DSC curves of PLA annealed at 90 and 100°C were shown in Figure 3. The small exothermal peak disappears, and an additional melting peak (T_{m2}) was observed in the form of a small shoulder (Figure 3a) that stretches

Sample	T_g (°C)	T_{cc} (°C)	ΔH_c (Jg^{-1})	T_m (°C)	ΔH_m (Jg^{-1})	X_c (%)
PLA-pellets	59.5	125.8	1.65	152.5	3.60	2.1
un-aPLA	60.0	127.2	3.41	153.4	4.86	1.6

Abbreviation: PLA, poly(lactic acid).

TABLE 1 Results from thermal analysis of PLA-pellets and un-aPLA sample

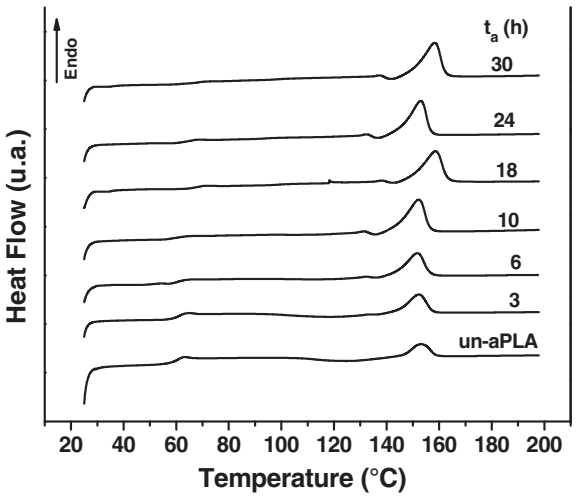

FIGURE 2 DSC curves of aPLA sheets at $T_a = 80°C$ for times $t_a = 3–30$ h

towards long annealing times in the case of aPLA ($T_a = 90°C$; t_a: 3–30 h). The two peaks, low-intensity T_{m2} (α' phase) and high-intensity T_{m1} (α phase), present a α'-α phase transition, with a α' phase in minority. In the case of annealing at 100°C (Figure 3b), the two peaks (T_{m2} and T_{m1}) appear for all annealing times (t_a: 3–30 h), thus showing a α'-α transition of phases with the same order of magnitude. Results of thermal properties of aPLA (T_a = 90,100°C; t_a: 3–30 h) samples are given in Table S1.

Samples annealed at $T_a = 110°C$ for $t_a = 3$ and 6 h show two peaks, T_{m2} of high intensity and T_{m1} as weak shoulder (Figure 4), indicating the presence of a α'-α phase transition. Annealing for $t_a = 10$ h yields to a single high-intensity T_{m2} peak indicating that the α' phase is completely transformed into the α phase. Results from thermal analysis of aPLA ($T_a = 110°C$; t_a: 3–30 h) are given in Table 3.

Figure 5 shows a single peak T_{m2} of high intensity when annealing at $T_a = 120°C$, thus indicating that the α' phase is wholly transformed into the α phase. Beyond $T_a = 120°C$, the α phase is perfectly established, as shown in Figure S1a, b, corresponding to PLA samples annealed at 130 and 140°C. Results of the thermal properties of samples annealed at T_a = 120, 130, and 140°C are given in Table S2.

3.2 | α'-α phase diagram

The α'-α phase diagram, built from temperatures of T_{exo}, T_{m1} and T_{m2} peaks, is of great interest to better understand the evolution of the crystal structure as function of t_a and T_a. Figure 6a gives a follow-up of α' and α as function of T_a for different t_a. The lower and upper limits of the α'-α phase transition require special attention. The lower limit of the α'-α transition coincides with the appearance of T_{m1} and T_{m2}; but often it is below 5 to 10°C since the α'-form transforms into α at T_{exo}. The upper limit is determined by linear extrapolation of T_{m2}, which is considered to correlate with the melting phenomenon of the α-form. Giving the equilibrium melting temperature (T_m^0) at $T_m = T_a$, the Hoffman-Weeks equation can be written as[39]:

$$T_m = T_m^0\left[1-\frac{1}{r}\right]+\frac{1}{r}T_a \quad (4)$$

where $1/r$ is the stability parameter depending on the crystal thickness, and r represents the ratio of the lamellar thickness at T_m to the lamellar thickness of the critical nucleus at T_a. Figure 6b shows the Hoffman-Weeks plots of aPLA, at 3 and 24 h for different T_a, showing the upper limits towards $T_a = 110°C$. The α'-α phase transition is therefore situated between 90 and 110°C with $T_m^0 = 168.3$ and 172.3°C for aPLA at t_a = 3 and 24 h, respectively. Table 4 reports T_m^0 and $1/r$ for aPLA at different times (t_a: 3–24 h).

Since α' crystals transform to α crystals upon heating, only annealing temperatures above $T_a \geq 110°C$ were considered, where the α crystals are predominantly produced. It has been firmly established that crystallization at high supercooling of the melt, defined by $\Delta T = T_m^0 - T_a$, allows the development of increasingly smaller nuclei of supercritical size than crystallization at low supercooling. The aPLA ($T_a = 80°C$; $t_a = 3$ h) sample clearly shows high supercooling ($\Delta T \approx 88°C$) compared to the aPLA ($T_a = 120°C$; $t_a = 24$ h) sample which presents low supercooling ($\Delta T \approx 52°C$). The aPLA ($T_a = 80°C$; $t_a = 3$ h) sample with high supercooling develops increasingly smaller nuclei of supercritical size.

The domain of the α'-α phase transition is often reported in the literature between 100 and 120°C,[25,29–31] which is highly desirable for molding and extrusion to

TABLE 2 Results from thermal analysis of annealed samples at $T_a = 80°C$ for $t_a = 3–30$ h

Sample	t_a (h)	T_g (°C)	T_{cc} (°C)	ΔH_c (Jg^{-1})	T_{exo} (°C)	T_{m1} (°C)	T_{m2} (°C)	ΔH_m (Jg^{-1})	X_c (%)
aPLA (80°C–t_a)	3	61.5	116.1	3.75	—	152.0	—	10.61	7.4
	6	62.1	118.0	0.85	—	153.1	—	13.81	13.9
	10	60.2	—	—	131.8	152.4	—	16.78	18.0
	18	63.5	—	—	132.9	152.8	—	17.43	18.7
	24	65.6	—	—	132.3	152.6	—	17.83	19.2
	30	62.7	—	—	131.9	152.4	—	17.84	19.2

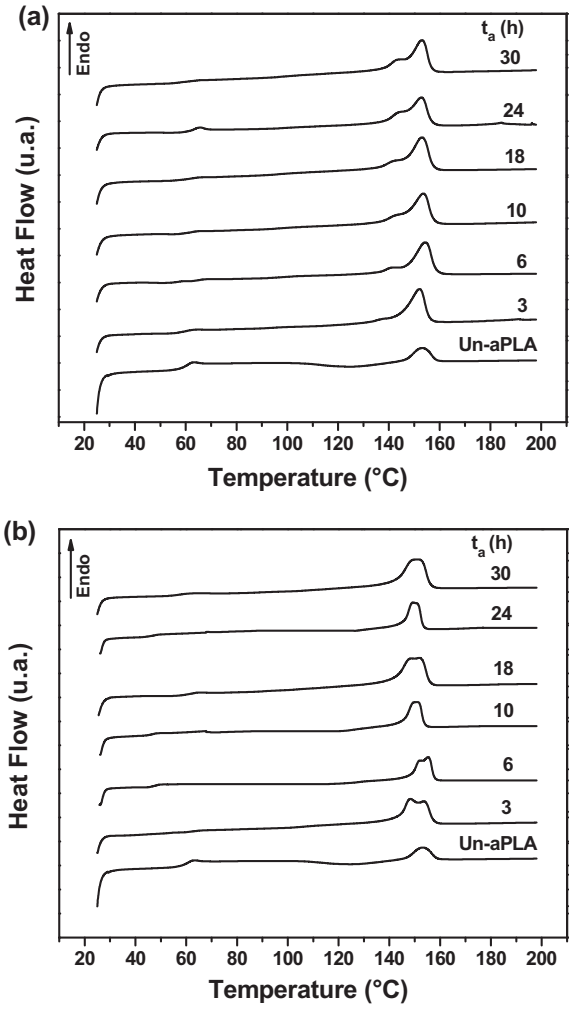

FIGURE 3 DSC curves of aPLA samples for times t_a: 3–30 h, at (a) $T_a = 90°C$ and (b) $T_a = 100°C$

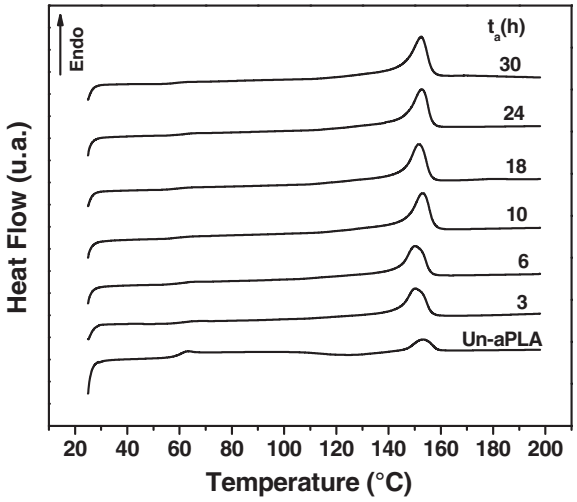

FIGURE 4 DSC curves of aPLA samples at $T_a = 110°C$ for t_a: 3–30 h

get optimal crystallinity. However, this domain is sometimes shifted towards lower or higher temperatures, strongly depending on heat treatment, molecular weight, external induced effects, and so forth. Jalali et al.[25] observed the domain of the α'-α phase transition between 100 and 120°C for PLA samples, exhibiting the highest crystallization temperature, the highest nuclei density, and the smallest spherulite size. Zhang et al.[29,30] showed that for PLA of molecular weight $M_w = 150{,}000$ g/mol, the α'-α phase transition is located at $110°C < T_c < 130°C$ while for low molecular weights ($M_w = 50{,}000$ g/mol), it was found around 105–130°C. Kawai et al.[31] showed that from melt-crystallization at $T_c = 80°C$, the peak T_{exo}, characterizing the α' phase, appears clearly for different heating rates from 1 to 20°C/min, and that the range of the α'-α phase transition can be estimated to be around 80–120°C. Pan et al.[23] found that the α'-α transition depends entirely on t_a (0–24 h) and T_a (120–160°C), and M_w affects the crystalline phase transition significantly, which can be explained by the mobility of polymer chains. Zhou et al.[40] studied deformational behavior and structural evolution of amorphous and aPLA samples stretched within 100–150°C. The amorphous PLA stretched at 120°C exhibits excellent mechanical properties.

The aPLA (T_a; t_a) sample, considered in this study, presents a α'-α phase transition around 90–110°C, as shown in Figure 6a that is slightly shifted towards lower temperatures, compared to the standard range 100–120°C.

TABLE 3 Thermal properties of annealed samples at $T_a = 110°C$ for t_a: 3–30 h

Sample	t_a (h)	T_g (°C)	T_{cc} (°C)	ΔH_c (Jg^{-1})	T_{exo} (°C)	T_{m1} (°C)	T_{m2} (°C)	ΔH_m (Jg^{-1})	X_c (%)
aPLA (110°C–t)	3	62.1	—	—	—	152.8	150.2	17.96	19.3
	6	62.1	—	—	—	151.6	150.1	19.17	20.6
	10	59	—	—	—	—	152.9	20.84	22.4
	18	59.3	—	—	—	—	151.5	21.17	22.7
	24	62.4	—	—	—	—	152.6	23.42	25.2
	30	59.4	—	—	—	—	152.4	23.67	25.4

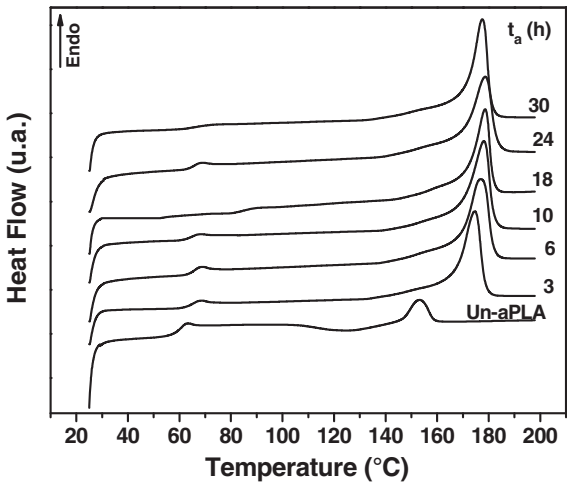

FIGURE 5 DSC curves of aPLA samples at $T_a = 120°C$ for annealed times (t_a = 3–30 h)

3.3 | Effect of annealing temperature and time on crystallinity

Figure 7 shows the effect of T_a for different times t_a on the crystallinity rate X_c, evaluated using Equation (2). At $T_a = 80°C$, samples annealed during 3 and 6 h exhibit $X_c = 7.4\%$ and 14.8% with a cold crystallization at 116 and 117°C, respectively. This is in good agreement with the work of Mijovićet al.,[41] Tsuji et al.[42] and Park et al.[43] where grain like morphology was observed during cold crystallization at 80°C. Annealing times of 3 and 6 h are not sufficient to achieve complete crystallinity which occurs at times t_a = 10–30 h around $X_c = 19\%$. For annealing temperatures in the range $80°C \leq T_a < 90°C$ at t_a: 10–30 h, the cold crystallinity disappears, and X_c shows plateau values around 19% (Figure 7), which can be explained by the presence of the disordered α' phase (see thermograms of Figure 2). For annealing temperatures in the range $90°C \leq T_a < 110°C$, the crystallinity begins to increase at 90°C with more substantial growth from 100°C up to 110°C ($X_c \approx 25\%$ for $T_a = 110°C$ at $t_a = 24$ h). For $T_a > 110°C$, X_c grows to reach an optimal crystallinity ($X_c \approx 32\%$) at 120°C. The domain of α'-α phase transition ($90°C \leq T_a < 110°C$), reported by the melting peaks T_m (Figure 6a), is shifted by approximately 10°C towards lower temperatures compared to that predicted by X_c versus T_a. In the latter case, above 110°C, X_c increases rapidly to an optimal value of 32% followed by a plateau above 120°C. On the other hand, the first case clearly shows a α'-α phase separation, with the presence of the two melting peaks limited to 110°C. The strong growth of X_c at $T_a > 110°C$ is due to discontinuities and

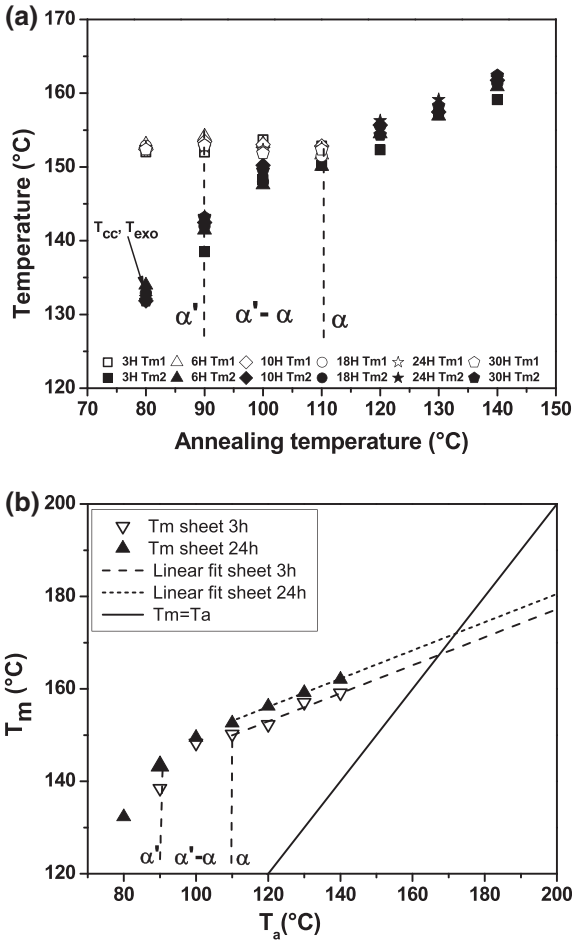

FIGURE 6 (a) Melting peaks T_{m1} and T_{m2} plotted as a function of T_a for t_a: 3–30 h; (b) Hoffman-Weeks plots for aPLA for 3 and 24 h at different temperatures

TABLE 4 Equilibrium melting temperature T_m^0 and stability parameter ($1/r$) for aPLA at different times

Samples	t_a (h)	T_m^0 (°C)	$1/r$	R^2
Hoffman-Weeks plots for annealed PLA for 3–24 h	3	168.3	0.314	0.96
	6	171.9	0.348	0.98
	10	169.7	0.284	0.96
	18	170.9	0.315	0.97
	24	172.3	0.312	0.99

Abbreviation: PLA, poly(lactic acid).

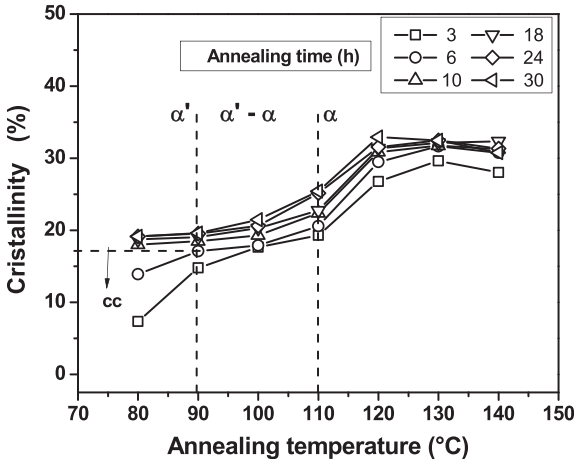

FIGURE 7 Crystallinity of aPLA as a function of temperature T_a for different times t_a

strong growth of the dimensions of the spherulites observed in the same temperature range, as already mentioned by several authors.[41–45] Mijovićet al.[41] showed a series of optical micrographs taken at different times during melt- and cold-crystallization at 140 and 80°C, respectively. The resulting morphologies are quite different; larger and more perfect spherulites were formed during melt-crystallization at 140°C whereas a grain like morphology was observed during cold crystallization at 80°C. Tsuji et al.[42] found that the radii of spherulites of melt-crystallized PLLA samples increased dramatically from 10 to 150 μm when the annealing temperature (T_a) was increased from 100 to 160°C. Park et al.[43] observed that density and size of spherulites increase with an increase of annealing time and temperature. For a semi-crystalline polymer, crystal growth rate is generally faster when T_a is close to its crystallization temperature.[43–45]

3.4 | Dynamic mechanical behavior

Figures 8 and 9 illustrate storage modulus E' and tan δ (defined as E''/E') of PLA sheet as function of temperature, for un-aPLA and aPLA (T_a: 80–140°C; t_a:3–24 h), respectively. The shape of E' thermograms (i.e., drop, rise, and drop) of un-aPLA and aPLA ($T_a = 80$°C; $t_a = 3,6$ h), is associated with the recrystallization process as given by Figure 8a,b. Above T_g, the increase of the chain mobility favors the crystallization process, which proceeds due to a slow scan rate (3°C/min) coupled with sinusoidal solicitation.

Incompletely crystallized samples show around 100°C an increase in E' ($T > T_g$), caused by the cold crystallization phenomenon. The recrystallization induces stiffening of the macromolecular chains, responsible for the increase of the storage modulus. Towards high temperatures, the storage modulus drops when the material starts to flow, corresponding to crystal melting of the material. The drop of E' values of un-aPLA and aPLA ($T_a = 80$°C; $t_a = 3$–6 h) samples is much faster than that in the case of highly crystallized aPLA (T_a: 90–140°C; $t_a = 3$–6 h) and aPLA (T_a: 80–140°C; $t_a = 10$–24 h) samples, which do not exhibit any further recrystallization process ($T > T_g$) and behave as perfectly semi-crystalline material. Thus, annealing, and therefore crystallization, can improve the heat resistance of PLA mainly due to restriction of molecular motion by the formation of firm spherulites.

The behavior of tan δ around T_g of un-aPLA and aPLA (T_a: 80–140°C; t_a: 3–24 h) are presented in Figure 9. The major relaxation process is associated with T_g, measured by the temperature of tan δ peak, where the sharpness and height are affected by the crystallinity. The un-aPLA sample behaves like an amorphous polymer showing a very sharp and intense tan δ peak because there is no restriction of the motion of the main chain. On the other hand, in semi-crystalline polymers, the dispersed crystalline regions hinder the chain mobility in the amorphous regions that is illustrated by a reduction of sharpness and height of the tan δ peak. A significant reduction of the height of the tan δ peak is observed for aPLA ($T_a = 80$°C; $t_a = 3$ h) (Figure 9a) with the same sharpness due to the low crystallinity ($X_c = 7.4\%$) and the presence of cold crystallinity. Tan δ of aPLA (T_a: 90–140°C; $t_a = 3$ h) is represented by a sharp enlargement with a decrease of peaks due to the increase in crystallinity (16.5% to 32.1%), thus showing the semi-crystalline behavior of these samples. Tan δ of aPLA (T_a: 80–140°C; t_a) samples annealed at 6, 10, and 24 h, shows

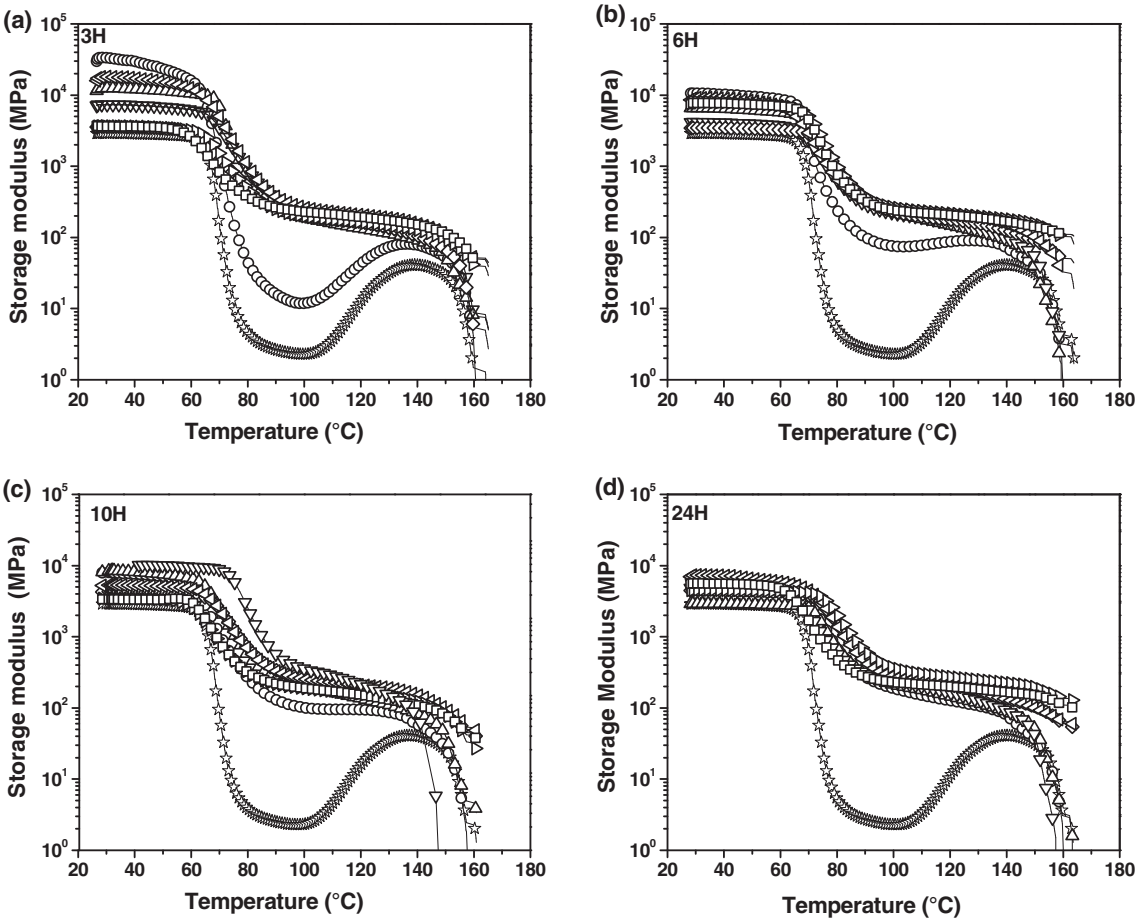

FIGURE 8 Storage moduli of un-aPLA and aPLA (T_a: 80–140°C; t_a) as a function of temperature for different annealing times. The symbols represent: ☆ Un-aPLA, ○ aPLA80, △ aPLA90, ▽ aPLA100, ◇ aPLA110, ◁ aPLA120, ▷ aPLA130, □ aPLA140

wide peaks with low amplitudes, thus characterizing a perfectly semi-crystalline behavior as shown in Figure 9b–d.

3.5 | Effects of annealing temperature and time on PLA stiffness

The salient fact, which emerges from thermograms of Figures 8 and 9, is the behavior of glassy moduli E_g and loss tan δ as function of annealing temperature T_a at different times t_a, observed for low temperatures and around the glass transition. T_g's of different aPLA (T_a; t_a) samples, illustrated in Table 5, show an increase for T_a (T_a: 90–110°C) and t_a (t_a: 3–24 h), thus presenting greater rigidity of the material, particularly for the sample annealed at $t_a = 24$ h with $T_g = 80.1$°C. The increase of T_g in the range T_a: 90–110°C is due to the growth of crystallinity as shown in Figure 7. This can be correlated with the α'-α phase transition domain (T_a: 90–110°C), given by DSC data in Figures 6 and 7, thus confirming the improvement of the stiffness of the material.[26,29–31]

The stiffness of aPLA (T_a; t_a) samples can be also viewed through the typical glassy plateau E_g (Figure 8), observed for all samples, depending on crystallinity and molecular weight. Given the same molecular weight, E_g should increase with crystallinity, but this trend was not observed. Indeed, PLA degrades due to thermal cleavage causing thus a substantial reduction of its molecular weight. This is an inevitable effect that must be taken into account when setting processing and annealing conditions of the material. Through monitoring E_g versus T_a at different t_a (Figure 10), two particular effects emerge from aPLA ($T_a = 80$°C; $t_a = 3$ h) and aPLA ($T_a = 120$°C; t_a): firstly, the very high value of E_g (29,900 MPa) of aPLA ($T_a = 80$°C; $t_a = 3$ h), and secondly the improvement of E_g around $T_a = 120$°C for all annealing times (t_a: 3–24 h). This improvement can be represented by the reduced glassy modulus E_{gR} equal to the ratio of the maximum modulus ($E_{gmax120}$) at $T_a = 120$°C and the maximum modulus (E_{gmax}) along the curve t_a ($E_{gR} = E_{gmax120}/E_{gmax}$). The sample annealed at $t_a = 24$ h presents the highest ratio ($E_{gR} = 0.9$), corresponding to a strong crystallinity generated by the couple (T_a, t_a), which will be elucidated

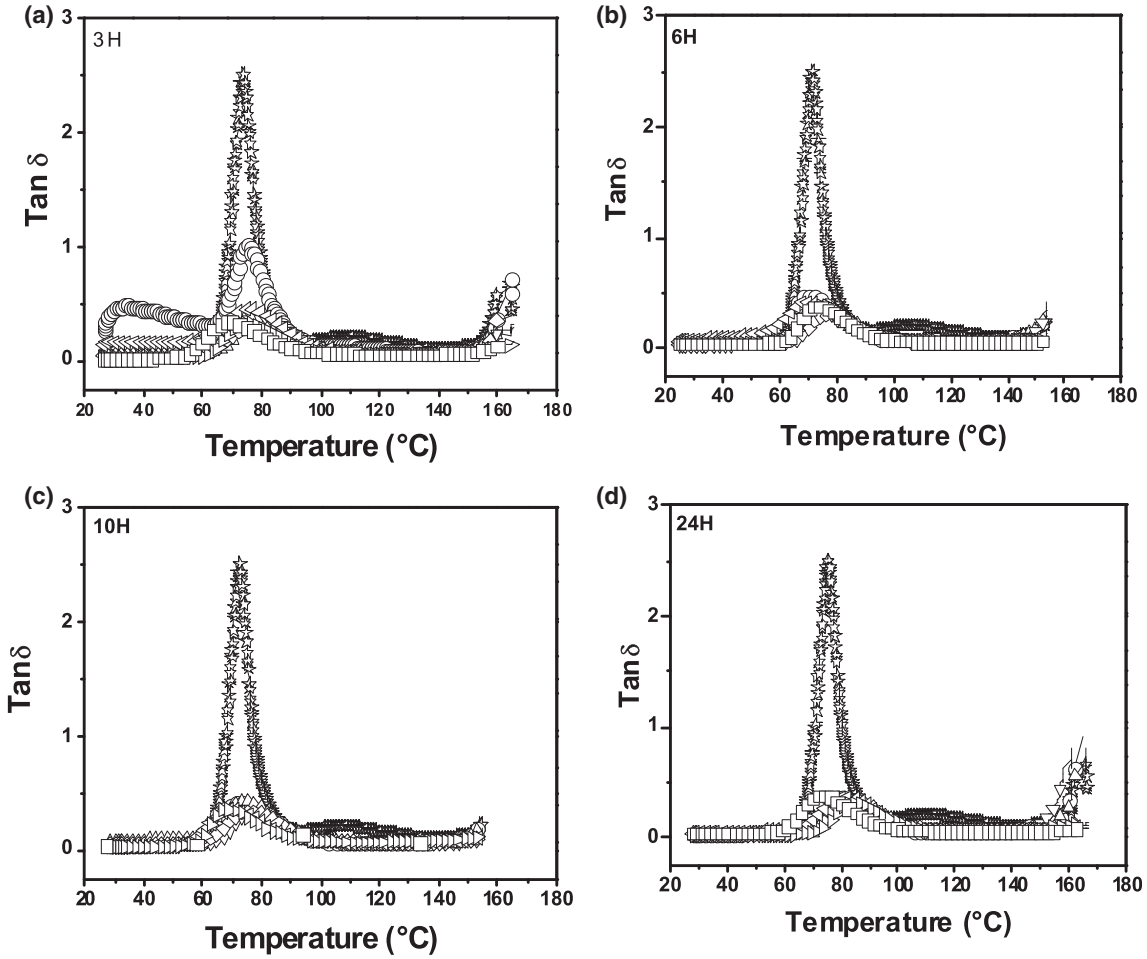

FIGURE 9 Tan δ of un-aPLA and aPLA (T_a: 80–140°C; t_a) as a function of temperature for different annealing times. The symbols represent: ☆ un-aPLA, ○ aPLA80, △ aPLA90, ▽ aPLA100, ◇ aPLA110, ◁ aPLA120 ▷ aPLA130, □ aPLA140

TABLE 5 DMA glass transition temperatures of aPLA (T_a: 80–140°C; t_a: 3–24 h). The T_g for un-aPLA corresponds to 75.2°C

Annealing temperature (°C)	T_g–3 h (°C)	T_g–6 h (°C)	T_g–10 h (°C)	T_g–24 h (°C)
80	74.8	73.6	71.9	77.6
90	75.6	77.5	76.9	79.3
100	77.3	79.5	76.1	75.0
110	77.8	78.1	76.8	80.1
120	73.5	73.9	75.7	76.0
130	73.6	74.3	73.6	77.3
140	68.6	71.9	71.1	71.2

Abbreviation: DMA, dynamic mechanical analysis.

in the next chapter. After a drop from $T_a = 80°C$, E_g begins to increase around $T_a = 110°C$ for all annealing times (t_a: 3–24 h), to reach a maximum value at $T_a = 120°C$, corresponding to the maximum of crystallinity (Figure 7).

This improvement in rigidity around $T_a = 120°C$, independently of t_a, corresponds to the (α'-α) phase separation, obtained from DSC data (Figures 6 and 7). This can be explained by the fact that despite a high T_a (120°C), which is supposed to reduce the rigidity of the material thermally, an improvement of the modulus E_g is observed in the range T_a: 100–120°C. This effect, linked to the (α'-α) phase transition, is highly sought after in the molding and extrusion of PLA type materials.

3.6 | Effects of crystallinity and molecular mass on aPLA ($T_a = 80°C$; t_a) and aPLA (T_a; $t_a = 24$ h) samples

Crystallinity and molecular weight M_v directly influence the behavior of the glass modulus. If crystallinity tends to increase E_g, decrease of M_v, on the other hand, tends to make it fall. To better understand these relationships, E_g, X_c, and M_v were determined as function of t_a and T_a, to

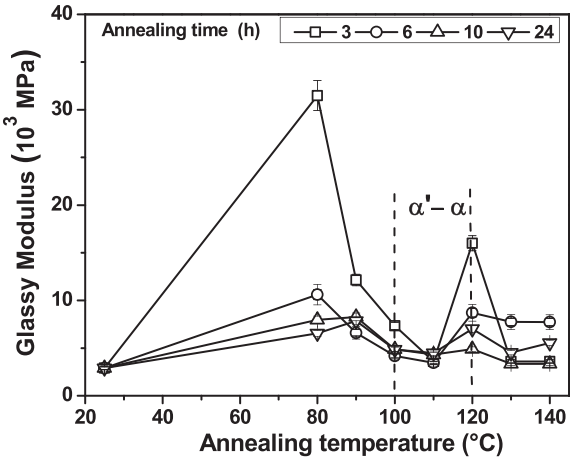

FIGURE 10 Glass modulus E_g of annealed PLA as a function of T_a for t_a: 3–24 h. E_{gR} of the t_a curves is 0.5, 0.8, 0.8 and 0.9 relative to annealing times 3, 6, 10 and 24 h, respectively

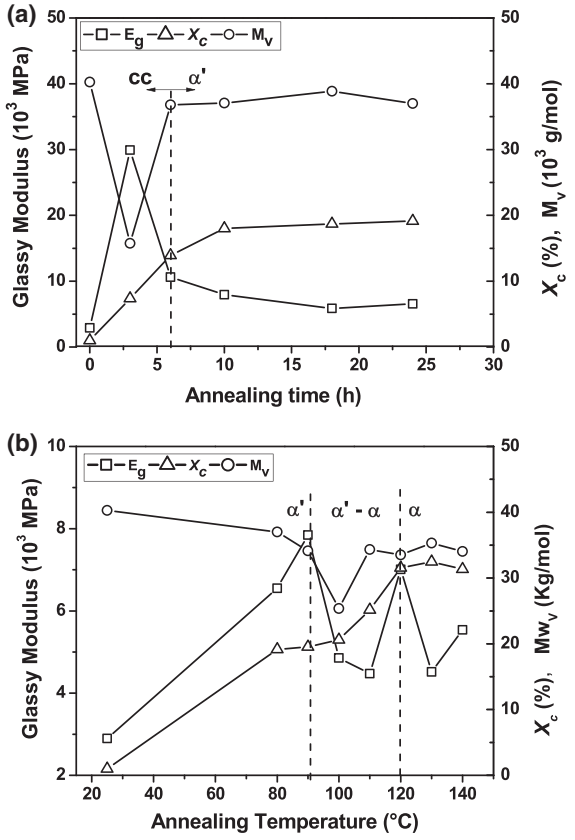

FIGURE 11 Glass modulus E_g, crystallinity X_c, and molecular weight M_v, as functions of (a) time t_a for $T_a = 80°C$; (b) temperature T_a for $t_a = 24$ h

analyze particular effects concerning aPLA ($T_a = 80°C$; $t_a = 3$ h) and aPLA ($T_a = 120°C$; $t_a = 24$ h) samples (Figure 10). Concerning the first sample, E_g suddenly increases from the un-annealed state (2900 MPa) up to 29,900 MPa at $t_a = 3$ h despite the drop of M_v from 40,200 to 15,700 g/mol (Figure 11a). Regarding crystallinity, the slight increase of X_c (~8%) cannot be the cause of this spectacular increase of the modulus. Indeed, structure and molecular mobility of the amorphous phase are strongly affected by the crystalline morphology developed in semi-crystalline polymers. The first indication comes from the theory of nucleation.[46–55] More particularly, a self-nucleation effect[47–51] could originate from smaller clusters or residual segmental orientation remaining in the melt, which play a role as precursors of the subsequent crystallization. From an industrial point of view, self-nucleation could be highly attractive to reduce time needed to process polymeric materials and to improve their final properties. The particularity of this process is that the critical size of the nucleus decreases with an increase in supercooling of the melt. Crystallization at high supercooling of the melt i.e. in the order of several tens of degrees, allows the development of increasingly smaller nuclei of supercritical size compared to crystallization at low supercooling. The aPLA ($T_a = 80°C$; $t_a = 3$ h) sample responds to this crystallization scheme with a high supercooling of the melt exhibiting $\left(T_m^0 - T_a\right) > 70°C$. An extremely high nucleation density in low crystallization PLA materials around 80°C has been highlighted.[34,50,51] The increase of the crystallization rate in the case of aPLA ($T_a = 80°C$; t_a) samples, shown in Figure 11a, can thus be attributed to self-nucleation.

The multitude of spherulites of nanometric dimensions resulting from strong nucleation are considered as crosslinking nodes, thus significantly increasing the material's rigidity. This explains the strong growth of E_g for aPLA ($T_a = 80°C$; $t_a = 3$ h). A decrease of E_g was observed for $t_a = 6$ h, beyond which it stabilizes around an average value of 8000 MPa. This proves that crystallinity strongly depends on t_a and that a critical time exists, corresponding to a critical size of the nucleus, followed by another growth domain of larger crystals.[45–51] The increase of E_g also results from cold crystallinity observed on the thermograms of the samples annealed at 3 and 6 h, given by DSC (Figure 2) and DMA (Figure 8b). Above $t_a = 10$ h cold crystallinity disappeared, and the fall of moduli, caused by the heat treatment, was damped by the increase of crystallinity (19%). Beyond $t_a = 10$ h, the different properties, E_g, M_v, and X_c, tend towards plateau values around 6500 MPa, 37,500 g/mol and 19%, respectively. The sudden increase of molecular weight beyond $t_a = 6$ h can be attributed to the crystallinity effect where larger-sized crystallites greatly limit chain mobility and prevent polymer degradation. Another interesting effect is the improvement of the thermo-mechanical properties of aPLA (T_a; t_a) samples around $T_a = 110°C$ (i.e., around α'-α phase separation), in

particular for the aPLA (T_a: 100–120°C; t_a = 24 h) sample. Figure 11b illustrates the evolution of E_g, M_v, and X_c, as function of T_a at t_a = 24 h. Between 80 and 90°C, the crystallinity (~19%) was sufficient to increase E_g (from 6500 to 7800 MPa) despite the drop of M_v (from 37,000 to 34,000 g/mol). Between 90 and 100°C, the strong decrease of M_v (from 34,000 to 25,000 g/mol) causes a strong drop of E_g (from 7800 to 4800 MPa), despite a slight increase of crystallinity. From 100 to 120°C, the strong increase of crystallinity (from 20% to 31.5%) directly led to an improvement of E_g (from 4800 to 7800 MPa), and an increase of M_v from 25,000 to 35,000 g/mol before stabilizing around 34,000 g/mol. This can be explained by the formation of large crystallites hindering chain mobility and, therefore, dramatically reducing the drop in molecular weight. The material exhibits optimal conditions around 120°C in terms of crystallinity (X_c = 31.5%), molecular weight (M_v = 35,000 g/mol) and rigidity (E_g = 7800 MPa), thus very favorable conditions for the production of semi-crystalline materials.

3.7 | Polymorphism in aPLA (T_a = 80°C; t_a) and aPLA (T_a; t_a = 24 h) samples

In terms of polymorphism, two domains can emerge for aPLA (T_a = 80°C; t_a: 3–24 h) (Figure 11a): the domain of self-nucleation below t_a = 6 h with a very high rigidity particularly at t_a = 3 h, and the domain of α'-crystals corresponding to the appearance of the T_{exo} peak beyond t_a = 6 h as described by the DSC thermograms in Figure 2. The α'-α transition region, showing an improvement of the glass modulus, is not accessible during 24 h, limited by the thermal stability of the material. For aPLA (T_a: 80–140°C; t_a = 24 h) (Figure 11b), the annealing temperature scan (T_a: 100–120°C) shows a strong increase of the crucial parameters E_g, X_c, and M_v, thus predicting the same effects (improvement of rigidity) as the α'-α phase separation in the range T_a: 90–110°C, determined by T_m's peaks (DSC, Figure 6). Below 90°C, the increase of modulus is mainly due to the extremely high nucleation density in PLA materials, what may be associated with the α' phase. For T_a: 90–110°C, a drop of the modulus was observed due to the decrease of M_v despite the strong crystallinity. Between 110 and 120°C the strong increase in crystallites induces a marked improvement of the modulus, limiting the movement of the chains and improving the mechanical properties of the polymer. Beyond 120°C, crystallinity and molecular weight stabilize, corresponding to the α phase.

4 | CONCLUSIONS

In the present report, the thermal behavior of various PLA samples annealed at various T_a and t_a's, were investigated by DSC and DMA measurements. It has been found that the small exothermic peak in the DSC curve just prior to the melting peak, associated with the (α'-α) phase transition, was detected at T_a = 80°C and $t_a \geq 10$ h. This phase separation, reported by the double T_m melting peak in the range T_a: 90–110°C, can be correlated with the increase of crystallinity for T_a: 100–120°C. DMA data show a sharp enlargement with a decrease of tan δ peaks of aPLA due to the increase in crystallinity, showing the semi-crystalline behavior of these samples. The salient fact of this work is the substantial growth (~30,000 MPa) of the glassy modulus at T_a = 80°C for t_a:3–6 h, due to strong nucleation. The second interesting effect is the improvement of E_g for T_a: 100–120°C, regardless of time t_a, which can be correlated to the increase of crystallinity in the range of T_a: 100–120°C, and the α'-α phase transition (T_a: 90–110°C).

AUTHOR CONTRIBUTIONS

Assia Zennaki: Investigation (lead). **Latifa Zair:** Investigation (supporting); visualization (equal). **Khadidja Arabeche:** Conceptualization (equal); data curation (equal); validation (equal). **Lina Benkraled:** Investigation (equal); visualization (equal). **Ulrich Maschke:** Writing – review and editing (equal). **Abdelkader Berrayah:** Conceptualization (equal); methodology (equal); supervision (equal); writing – original draft (equal).

ACKNOWLEDGMENTS

The authors gratefully acknowledge the support of the Algerian Ministry of Higher Education and Scientific Research (MESRS), the General Directorate of Scientific Research and Technological Development (DGRSDT) of Algeria, the University of Tlemcen/Algeria, the CNRS, and the University of Lille/France.

CONFLICT OF INTEREST

The authors declare that they have no known competing financial interests or personal relationships that could have appeared to influence the work reported in this paper.

DATA AVAILABILITY STATEMENT

The data that support the findings of this study are available on request from the corresponding author.

ORCID

Ulrich Maschke https://orcid.org/0000-0001-7970-1966

REFERENCES

[1] L. T. Lim, R. Auras, M. Rubino, *Prog. Polym. Sci.* **2008**, *33*, 820.
[2] C. K. Williams, M. A. Hillmyer, *Polym. Rev.* **2008**, *48*, 1.
[3] R. P. Babu, K. O'Connor, R. Seeram, *Prog. Biomater.* **2013**, *2*, 8.
[4] R. Auras, B. Harte, S. Selke, *Macromol. Biosci.* **2004**, *4*, 835.
[5] Z. Kulinski, E. Piorkowska, *Polymer* **2005**, *46*, 10290.
[6] S. M. Satti, A. A. Shah, T. L. Marsh, R. Auras, *J. Polym. Environ.* **2018**, *26*, 3848.
[7] W. S. Chow, E. L. Teoh, J. Karger-Kocsis, *Express Polym. Lett.* **2018**, *12*, 396.
[8] L. Cartier, T. Okihara, Y. Ikada, H. Tsuji, J. Puiggali, B. Lotz, *Polymer* **2000**, *41*, 8909.
[9] J. Puiggali, Y. Ikada, H. Tsuji, L. Cartier, T. Okihara, B. Lotz, *Polymer* **2000**, *41*, 8921.
[10] P. C. Dartora, M. da Rosa Loureiro, M. M. de Camargo Forte, *J. Therm. Anal. Calorim.* **2018**, *134*, 1705.
[11] T. Tábi, S. Hajba, J. G. Kovács, *J. Therm. Anal. Calorim.* **2019**, *138*, 1287.
[12] H. Simmons, P. Tiwary, J. E. Colwell, M. Kontopoulou, *Polym. Degrad. Stab.* **2019**, *166*, 248.
[13] L. Deng, C. Xu, X. Wang, Z. Wang, *Chem. Eng.* **2018**, *28*, 480.
[14] J. Chen, C. Deng, R. Hong, Q. Fu, J. Zhang, *J.Polym. Res.* **2020**, *27*, 1.
[15] E. Silva Barbosa Ferreira, C. B. B. Luna, D. D. Siqueira, E. M. Araújo, D. de Campos França, R. M. Ramo Wellen, *J. Polym. Environ.* **2022**, *30*, 541.
[16] P. Agrawal, A. P. Araujo, J. C. Lima, S. N. Cavalcanti, D. M. Freitas, G. M. Farias, M. M. Ueki, T. J. Melo, *J. Polym. Environ.* **2019**, *27*, 1439.
[17] M. Barletta, M. Puopolo, *J. Polym. Environ.* **2019**, *27*, 2105.
[18] P. de Santis, A. Kovacs, *Biopolymers* **1968**, *6*, 299.
[19] W. Hoogsten, A. R. Postema, A. J. Pennings, G. Ten Brinke, P. Zugenmaier, *Macromolecules* **1990**, *23*, 634.
[20] B. Kalb, A. J. Pennings, *Polymer* **1980**, *21*, 607.
[21] P. Pan, W. Kai, B. Zhu, T. Dong, Y. Inoue, *Macromolecules* **2007**, *40*, 6898.
[22] P. Pan, B. Zhu, W. Kai, T. Dong, Y. Inoue, *Macromolecules* **2008**, *41*, 4296.
[23] P. Pan, Y. Inoue, *Prog. Polym. Sci.* **2009**, *34*, 605.
[24] T. Tábi, S. Hajba, J. G. Kovács, *Eur. Polym. J.* **2016**, *82*, 232.
[25] A. Jalali, M. A. Huneault, S. Elkoun, *J. Mater. Sci.* **2016**, *51*, 7768.
[26] M. Di Lorenzo, P. Rubino, B. Immirzi, R. Luijkx, M. Hélou, R. Androsch, *Colloid Polym. Sci.* **2015**, *293*, 2459.
[27] C. Aleman, B. Lotz, J. Puiggali, *Macromolecules* **2001**, *34*, 4795.
[28] S. Sasaki, T. Asakura, *Macromolecules* **2003**, *36*, 8385.
[29] J. M. Zhang, Y. Duan, H. Sato, H. Tsuji, I. Noda, S. Yan, Y. Ozaki, *Macromolecules* **2005**, *38*, 8012.
[30] J. M. Zhang, K. Tashiro, H. Tsuji, A. J. Domb, *Macromolecules* **2008**, *41*, 1352.
[31] T. Kawai, N. Rahman, G. Matsuba, K. Nishida, T. Kanaya, M. Nakano, H. Okamoto, J. Kawada, A. Usuki, N. Honma, K. Nakajima, M. Matsuda, *Macromolecules* **2007**, *40*, 9463.
[32] M. Cocca, R. Androsch, M. C. Righetti, M. Malinconico, M. L. Di Lorenzo, *J. Mol. Struct.* **2014**, *1078*, 114.
[33] Y. Ohtani, K. Okumura, A. Kawaguchi, *J. Macromol. Sci., Part B: Phys.* **2003**, *42*, 875.
[34] T.-Y. Cho, G. Strobl, *Polymer* **2006**, *47*, 1036.
[35] Y. Zhao, Z. Qiu, S. Yan, W. Yang, *Polym. Eng. Sci.* **2011**, *51*, 1564.
[36] A. Schindler, D. Harper, *J. Polym. Sci.* **1979**, *97*, 2593.
[37] H. Tsuji, Y. Ikada, *Polymer* **1996**, *37*, 595.
[38] E. W. Fischer, H. J. Sterzel, G. Wegner, Z. Z. Kolloid, *Polym* **1973**, *251*, 980.
[39] J. D. Hoffman, J. J. Weeks, *J. Res. Natl. Inst. Stand. A Phys. Chem.* **1962**, *66*, 13.
[40] C. Zhou, H. Li, W. Zhang, J. Li, S. Huang, Y. Meng, J. D. Christiansen, D. Yu, Z. Wu, S. Jiang, *Polymer* **2016**, *90*, 111.
[41] J. Mijović, J.-W. Sy, *Macromolecules* **2002**, *35*, 63.
[42] H. Tsuji, Y. Ikada, *Polymer* **1995**, *36*, 2709.
[43] S. D. Park, M. Todo, K. Arakawa, M. Koganemaru, *Polymer* **2006**, *47*, 1357.
[44] H. D. Keith, F. J. Padden, *J. Appl. Phys.* **1963**, *35*, 1286.
[45] J. L. Way, J. R. Atkinson, J. Nutting, *J. Mater. Sci.* **1974**, *9*, 293.
[46] Y. Xu, Y. Wang, T. Xu, J. Zhang, C. Liu, C. Shen, *Polym. Testing* **2014**, *37*, 179.
[47] R. M. Michell, A. Mugica, M. Zubitur, A. J. Müller, in *Polymer Crystallization I*. Vol. 276 (Eds: F. Auriemma, G. Alfonso, C. de Rosa), Springer, Cham **2015**. https://doi.org/10.1007/12_2015_327
[48] L. Sangroniz, D. Cavallo, A. J. Müller, *Macromolecules* **2020**, *53*, 4581.
[49] B. Fillon, J. C. Wittmann, B. Lotz, A. Thierry, *J. Polym. Sci., Part B: Polym. Phys.* **1993**, *31*, 1383.
[50] A. T. Lorenzo, M. Arnal, J. J. Sánchez, A. J. Müller, *J. Polym. Sci., Part B: Polym. Phys.* **2006**, *44*, 1738.
[51] J. Jiang, E. Zhuravlev, W. B. Hu, C. Schick, D. S. Zhou, *Chin. J. Polym. Sci.* **2017**, *35*, 1009.
[52] M. L. Di Lorenzo, P. Rubino, R. Luijkx, M. Hélou, *Coll. Polym. Sci.* **2014**, *292*, 399.
[53] R. Androsch, C. Schick, *Adv. Polym. Sci.* **2015**, *276*, 257.
[54] X. Li, F. Su, Y. Ji, N. Tian, J. Lu, Z. Wang, Z. Qi, L. Li, *Soft Matter* **2013**, *9*, 8579.
[55] A. Martinelli, M. Calì, L. D'Ilario, I. Francolini, A. Piozzi, *J. Appl. Polym. Sci.* **2011**, *121*, 3368.

SUPPORTING INFORMATION

Additional supporting information can be found online in the Supporting Information section at the end of this article.

How to cite this article: A. Zennaki, L. Zair, K. Arabeche, L. Benkraled, U. Maschke, A. Berrayah, *J. Appl. Polym. Sci.* **2022**, e53095. https://doi.org/10.1002/app.53095